



Design of Metal Insulator Metal based Square Ring Resonator Plasmonic Filter using Silica Slits for Dual Band Applications

Surendra Kumar Bitra* and Sridhar M

Department of ECE, KoneruLakshmaiah Educational Foundation, Vaddeswaram, Guntur District, India

Received 13 October 2019; revised 18 March 2020; accepted 11 June 2020

In this paper, Metal-Insulator-Metal (MIM) based dual-band plasmonic bandpass filters (BPF) with single and dual silica slits design and analysis is presented. The Square Ring Resonator (SRR) is coupled using Coupled feed line for dual-band operations. The coupled feed line is used for dual-band operating wavelengths, 1300 nm (230.6 THz) and 1600 nm (187.37 THz). Design and simulations are performed using complex electromagnetic simulator known as computer simulation technology (CST) microwave tool. The proposed filters are used for plasmonic single and dual-band bandpass filter (BPF) applications in photonic integrated circuits (PIC's).

Keywords: BPF, MIM, Photonic Integrated Circuits, SRR

Introduction

Light interaction with the metal and dielectric interface forms a Surface Plasmon Polarities (SPP). These are electro-magnetic waves which are observed in the region of interface of metal and dielectric.^{1,2} SPP are excited and propagate along the surface of a metal with shorter wavelength³ which are much better than electromagnetic waves.⁴ Several nanoscale components based on plasmonic are proved to be capable of providing null bend losses while capable of low cost and low complexity in prototyping.^{5,18} MIM based rectangular ring resonator band pass filter is design and analysed using coupling gaps between input and output ports are implemented.^{12,13} Recently proposed different filters like ring resonators^{14,15}, tooth-shaped¹⁶ and Bragg gratings¹⁷ type. The merit of high transmission at 90° bends rectangular ring resonators are advantageous than circular ring resonator¹⁸ due to ease of fabrication. In this paper, MIM based waveguide structure is developed for dual-band applications and the effect of the geometrical transforms are analyzed.

Experimental Details

Modelling of MIM Waveguide

In MIM waveguide the insulator is sandwiched between two metal waveguides. The silica ($\epsilon_i = 2.50$) is used as the insulator and silver is used as metal.

The dielectric constant of the silver is expressed by the Drude model.¹⁹

$$\epsilon(\omega) = \epsilon_{\infty} - \frac{\omega_p^2}{\omega(\omega + j\gamma)} \quad \dots (1)$$

Where ($\epsilon_{\infty} = 3.7$) is permittivity of the metal, $\omega_p (= 1.38 \times 10^{16})$ is the plasma frequency and $\gamma (= 2.73 \times 10^{13})$ rad/sec is the damping frequency of the metal. Several nanoscale components like plasmonic based waveguides⁵, light-emitting devices⁶, solar cells⁷, V grooves⁸ and plasmon slots⁹ have been used in literature. However, some of the above-mentioned shapes are capable at nanoscale as they can concentrate the optical radiation to the core of the MIM. In addition, the MIM waveguides are essentially validated using several complex numerical simulations and experimentations. It is reported that these are capable of providing almost null bend losses while capable of low cost and low complexity in prototyping.^{10,11} The MIM waveguide is designed, simulated and analysed using FDTD (Finite Difference Time Domain Solver) based CST (Computer Simulation Technology) Microwave Studio Suite. The PML (Perfect Matched Layer) boundaries are used to investigate the waveguide and the mesh sizes are taken as 5 nm x 5 nm. Blue colour indicates Metal and gray colour indicates insulator throughout the paper.

Results and Discussion

Dual Band Filter without Silica Slits

The dual-band SRR is shown in Fig. 1 (a). The length of the SRR is $4 \times L_1 = 980$ nm, thickness of the

*Author for Correspondence
E-mail: bitrasurendrakumar@gmail.com

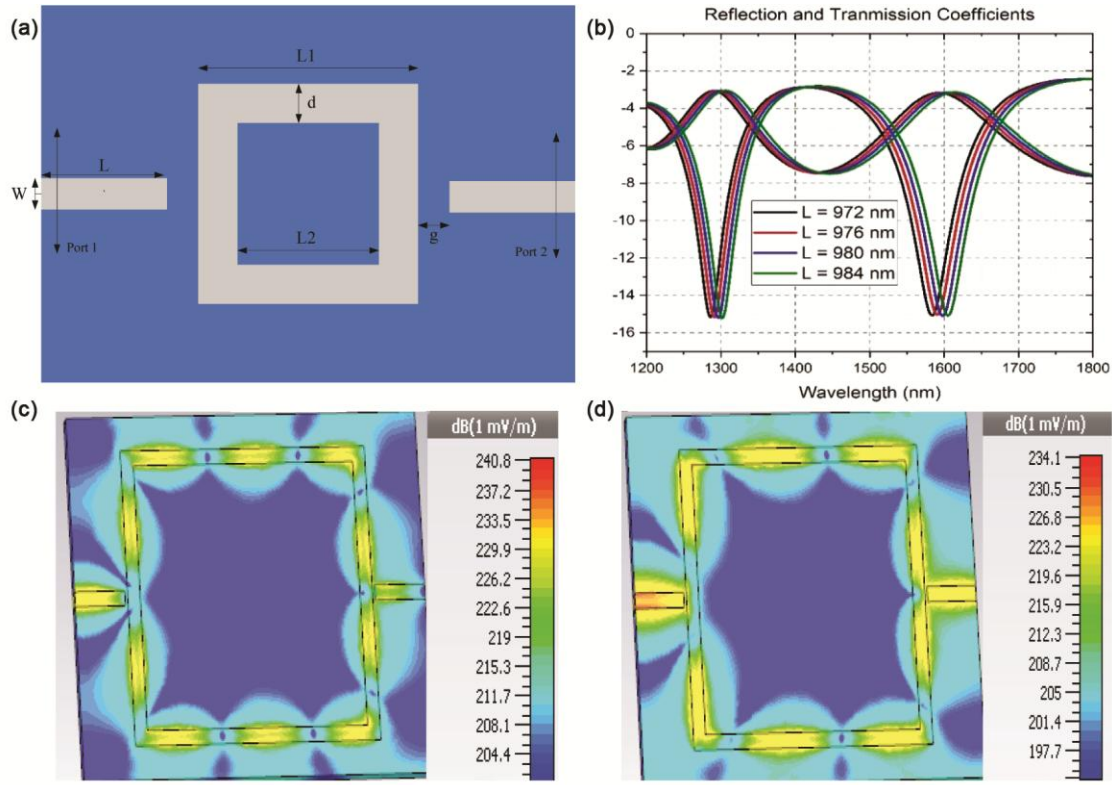


Fig. 1 — (a) Dual band SRR (b) Reflection and Transmission Coefficients of the rectangular Dual band SRR (c) Field distribution at 1300 nm (230.6 THz) and (d) 1600 nm (187.37 THz)

ring (d) is 50 nm. The coupled line feed is used for giving input power to the square ring.¹⁵ The gap (g) between feed and square ring is 10 nm. The width (W) of the coupled line feed is 50 nm and length (L) of coupled line feed is 100 nm. The resonance condition for the square ring cavity.^{12,15}

In order to study the effect of the cavity length on the characteristics of the filter the corresponding wavelength response curves have to be plotted for several cavity lengths. Such characteristic plot is given in Fig. 1(b). It is evident from Fig. 1(b) that the first and second valleys of reflection coefficients are shifted by varying the cavity lengths. The first and second valleys of reflection coefficients are linearly tuned by varying the cavity lengths. Accordingly, when the cavity length is enhanced the corresponding resonant wavelength is also enhanced. This is given in the following equation.

$$L = N\lambda_{SPP} = N(\lambda/Re(N_{eff})) \quad \dots (2)$$

Where, L is the rectangular cavity length, N is the resonance wavelengths ($N=1,2,3, \dots$). The dual-band SRR operates on 1300 nm (230.6 THz) and 1600 nm

(187.37 THz) wavelengths respectively. The field distributions of the dual band SRR at 1300 nm and 1600 nm are shown in Fig. 1 (c) and (d).

Dual Band Filter with single Silica Slits

The transmission characteristics of the MIM waveguide based SRR with a one silica slit or gap has been carried out by using CST microwave studio suite with the fixed widths of the waveguide and cavity as shown in the Fig. 2 (a). The variation in transmission spectra of the proposed SRR with single slit or gap ($g_1 = 2$ nm) as a function of wavelength for wide band light are shown in Fig. 2(b). The first resonant peak occurred at 1282 nm and second resonant peak occurs at 1598 nm wavelength respectively with a transmission loss of 14.3 dB and 15.8 dB wavelength respectively. If the length of the SRR increases, the transmission spectrum shifted to right side of the graph, the resonant wavelength of the first peak shifted from 1282 nm to 1300 nm and 1598 nm to 1605 nm respectively. The field distributions at 1282 nm and 1598 nm wavelengths respectively are presented Fig. 2(c) and (d).

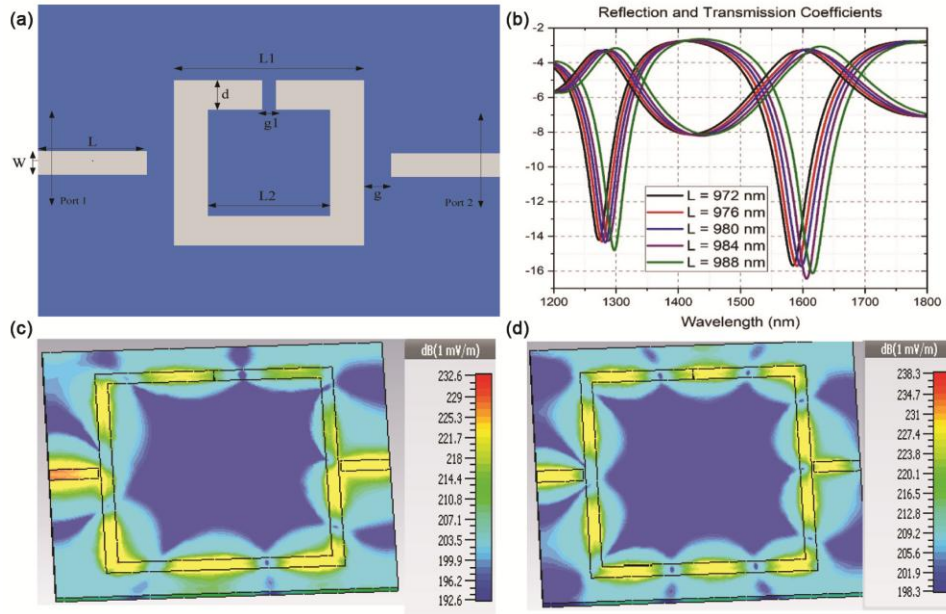


Fig. 2 — (a) Dual Band SRR using Single Slit (b) Reflection and Transmission Coefficients of Dual band SRR with Single Slit (c) Field Distribution in the Dual band SRR with single slit at 1282 nm (233.8 THz) (d) 1598 nm and (187.60 THz)

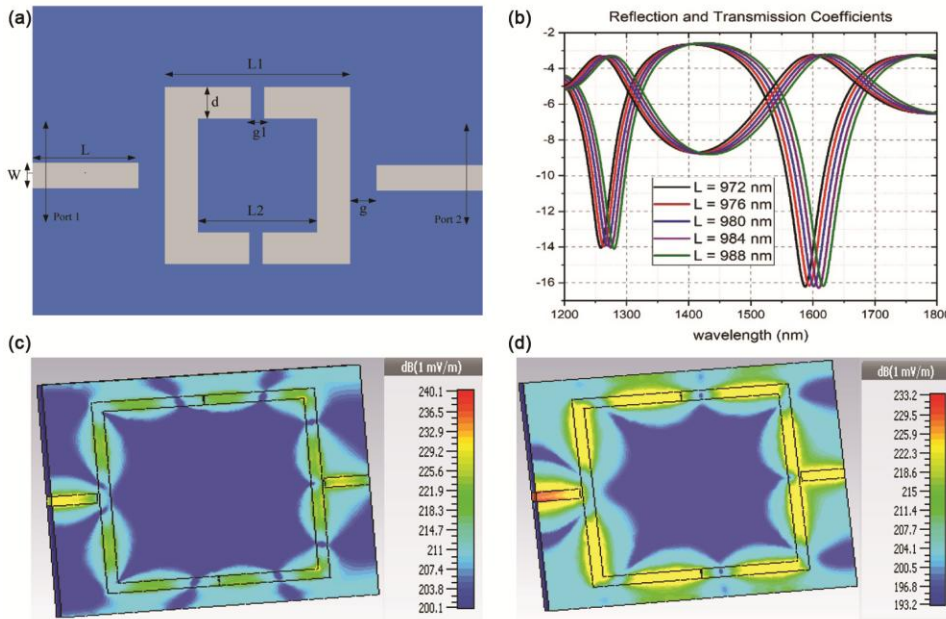


Fig. 3 — (a) Dual band SRR using Double Slits (b) Reflection and Transmission Coefficients of Dual band SRR using Double Slit (c)Field Distribution in the Dual band SRR with Double slits at 1270 nm (230.057 THz) and (d) 1601 nm (187.253 THz)

Dual Band Filter with Double Silica Slits

The transmission characteristics of the MIM waveguide based SRR with double slits or gaps at upper and lower sides has been carried out by using CST microwave studio suite with the fixed width of the waveguide and cavity respectively and the proposed filter is shown in Fig 3 (a). The variation in

transmission spectra of the proposed device of SRR with dual slits are shown in Fig. 3(b). The first resonant peak occurred at 1270 nm and second resonant peak occurs at 1601 nm wavelength respectively with a transmission loss of 14 dB and 16.2 dB respectively. If the length of the SRR increases, the transmission spectrum can be shifted

to right side of the graph. The field distributions at 1270 nm and 1601 nm wavelengths respectively are shown in Fig. 3(c) and 3(d).

Conclusions

The Dual band SRR plasmonic filters are simulated and numerically analysed. The length of the square ring 980 nm for dual-band filters. The square ring resonators are chosen due to ease of fabrication. The dual-band filters are designed to operate in 1300 nm (230.6 THz) and 1600 nm (187.37 THz) wavelengths respectively. These devices have designed, simulated and observed that the losses are increased with the increase of number of slits or gaps of the SRR. All the proposed dual band nature at optical frequency bands first resonant peak and second resonant peak are operated simultaneously at 1300 nm and 1600 nm respectively. All the dual band devices have band pass filter characteristics. The proposed resonate filter transmission characteristics are a good agreement with theoretical calculations. The single and dual-band BPF are used mainly in photonic integrated optical circuits.

References

- 1 Ozbay E, Plasmonics: Merging photonics and electronics at nanoscale dimensions, *Science*, **311** (2006) 189–193.
- 2 Atwater H A, The Promise of Plasmonics, *Sci Am*, **296**(4) (2007) 56–63.
- 3 Barnes W L, Dereux A & Ebbesen T W, Surface plasmon subwavelength optics, *Nature* **424**(8) (2003) 824–830.
- 4 Wassel H M G, Dai D, Tiwari M, Valamehr J K, Theogarajan L, Dionne J, Chong F T & Sherwood T, Opportunities and challenges of using plasmonic components in nanophotonic architectures, *IEEE J Emerg Sel Top Circuits Syst*, **2**(2) (2012) 154–168.
- 5 Keleshtery M H, Mir A & Kaatuzian H, Investigating the characteristics of a double circular ring resonators slow light device based on the plasmonics-induced transparency coupled with metal-dielectric-metal waveguide system, *Plasmonics*, **13**(4) (2017) 1523–1534.
- 6 Keleshtery M H, Kaatuzian H, Mir A & Zandi A, Method proposing a slow light ring resonator structure coupled with a metal-dielectric-metal waveguide system based on plasmonic induced transparency, *Appl opt*, **56**(15) (2017) 4496–4504.
- 7 Chou Chau Y F, Chou Chao C T, Huang H J, Kumara N T R N, Lim C M & Chiang H P, Ultra high refractive index sensing structure based on a Metal insulator metal waveguide coupled T shape cavity metal nanorod defects, *nanomaterials*, **9**(10) (2019) 1–14.
- 8 Yin J, Tian J & Yang R, Investigation of the transmission properties of a plasmonic MIM waveguide coupled with two ring resonators, *Material Research Express*, **6**(3) (2018) 1–16.
- 9 Xiong C, Li H, Zhao M, Zhang B, Liu C & Wu K, Coupling effects in single mode and multimode resonator coupled system, *Optic Exp*, **27**(13) (2019) 17718–17728.
- 10 Zhang Z, Luo L, Xue Ch, Zhang W & Yan S, Fano resonance based on Metal insulator metal waveguide coupled double rectangular cavities for plasmonic nanosensors, *Sensors*, **16**(5) (2016) 1–10.
- 11 Veronis G & Fan S, Bends and splitters in metal-dielectric-metal subwavelength plasmonic waveguides, *Appl Phys Lett*, **87**(13) (2005) 1–3.
- 12 Hosseini A & Massoud Y, Nanoscale surface plasmon based resonator using rectangular geometry, *Appl Phys Lett*, **90**(18) (2007) 2–5.
- 13 Banerjee S, Simulation and design of MIM nanoresonators for color filter applications, *J Soc Inf Disp*, **24**(7) (2016) 433–438.
- 14 Liu D, Sun Y, Fan Q, Mei M, Wang J, Yue-Wu P & Jian L, Tunable plasmonically induced Transparency with Asymmetric Multi-rectangle Resonators, *Plasmonics*, **11** (2016) 1621–1628.
- 15 Wang T B, Wen X W, Yin C P & Wang H Z, The transmission characteristics of Surface plasmon polaritons in ring resonators, *Optics Express*, **17**(26) (2009) 24096–24101.
- 16 Yang L, Li P, Wang H & Li Z, Surface plasmon polariton waveguides with subwavelength confinement, *Chin Phys B*, **27**(9) (2018) 094216–15.
- 17 Valentina D, Ahmed S, Jonas F, Samantha M, Sahba Talebi F & Lukas Ch, Design and fabrication of SoI micro-ring resonators based on sub-wavelength grating waveguides, *optic exp*, **23**(4) (2015) 4791–4803.
- 18 Rahman M Z U, Krishna K M, Reddy K K, Babu M V, Mirza S S, & Fathima S Y, Ultra-Wide-Band Band-Pass Filters Using Plasmonic MIM Waveguide-Based Ring Resonators, *IEEE Photonics Technol Lett*, **30**(19) (2018) 1715–1718.
- 19 Maier SA, *Plasmonics: Fundamentals and Applications* (Springer science-business media LLC), 2007, 1–104.